ASM Sc. J., 18, 2023

https://doi.org/10.32802/asmscj.2023.1477

Enhancing Thermal Performance of Evacuated Tube Solar Collector using Novel Graphene Oxide Nanofluid

S.S. Surve[1*], R.S.N. Sahai[1] and N.R. Jha[2]

[1]*Department of General Engineering, Institute of Chemical Technology, Mumbai, India*

[2]*Department of Physics, Institute of Chemical Technology, Mumbai, India*

The research article investigates the thermal performance of heat pipe-based evacuated tube solar collector (ETSC) experimentally using graphene oxide (GO) and deionised (DI) water as working fluid with a mass flow rate of 0.5 lit/min, 0.75 lit/min, and 1 lit/min. The different volumetric concentrations of 0.001%, 0.002%, and 0.003% graphene oxide nanofluid samples were prepared in the deionised water. The X-ray diffraction (XRD) was used to determine the structural properties of graphene oxide and the morphology of graphene oxide was studied by scanning electron microscope (SEM). To evaluate the stability of nanofluid samples, the Zeta potential analysis was carried out which showed that prepared nanofluid samples remain stable for up to 30 days. The effect of different nanofluid concentrations on various thermo physical properties of nanofluid was studied and discussed. The thermal performance of ETSC was investigated by considering the effect of volumetric concentrations of nanofluid and mass flow rates. According to the findings, there is a significant increment in temperature difference and energy gain by using nanofluid samples, and the maximum thermal efficiency of ETSC was found to be 37.1% for a volumetric concentration of 0.003% at 1 lit/min mass flow rate as compared to water.

Keywords: Nanofluid; Evacuated tube; Graphene oxide; Solar collector; Thermal efficiency

I. INTRODUCTION

Solar energy is the future of humanity as it is free and clean; hence it has been widely used to provide the required energy for daily usage with different techniques. Solar water heating with the solar collector is the most efficient method to use available solar energy but in conventional solar collectors, the absorber plate is occupied by a number of tubes, and water is a working medium that transfers the heat to the storage tank. This system required more space, less heat capacity, and a high heat loss factor. This problem leads to increased use of heat pipes with evacuated glass tubes.

The heat pipe mainly consists of a heating section, condensation section, wicked material, and a small quantity of working fluid. The working fluid gets vaporised in the heating section and condensates later into the condenser section, transferring the heat from the hot point to the cold point with the help of capillary action (Jouhara *et al.,* 2017). The various types of solar collectors have been used by many researchers however, heat pipe solar collectors (HPSC) with evacuated tubes are more efficient than other collectors as they have lower thermal resistance and very high thermal conductivity (Shafieian *et al.,* 2020). The study of Zheng *et al.* (2022) compared solar water heaters by calculating their efficiencies which showed that HPSC has minimum heat loss and better thermal efficiency. A comparison study of HPSC and flat plate solar collector (FPSC) reported by Tsai *et al.* (2011) confirmed that HPSC shows higher thermal efficiency over FPSC under similar conditions. However, a similar experiment performed on different types of the solar collector by Lee *et al.* (2021) concluded that the thermal efficiency of HPSC is more as compared to FPSC. The performance of solar collectors greatly depends on the type

*Corresponding author's e-mail: sssurve1987@gmail.com

of working fluid used in the study (Wole-osho *et al.,* 2020). Therefore, there are various fluids used by researchers in research papers to enhance the thermal characteristics of solar collectors. The experiment performed on the use of R134a and distilled water as working fluid in HPSC by Jayanthi *et al.* (2020) under various operating conditions showed that the thermal efficiency of HPSC increases significantly. A similar study of magnesium oxide (MgO) as nanofluid in HPSC gives significant enhancement in results in terms of thermal efficiency as reported by Dehaj and Mohiabadi (2019) also, by increasing coolant flow rate, the solar collector's thermal efficiency increases. The evacuated tube heat pipe is the most vital type of collector as it shows great performance all over the year even in minimum solar radiation. The experiment performed on finding the thermal efficiency of heat pipe with ETSC and U-tube ETSC by Sabiha *et al.* (2015) showed that heat pipe with ETSC has 8 % more thermal efficiency than U-tube ETSC.

Nanofluids are widely used as working fluid in solar collectors because it enhances the thermal characteristics of a solar collector (Ahmed *et al.,* 2019). In nanofluid, the metal or metal oxide particles having a diameter less than 100 nm mix with water to get maximum performance from solar collectors. However, only using water as an operative fluid in solar collectors leads to lower thermal efficiency (Kadhim & Ibrahim, 2021). Further, this efficiency can be increased by modification in design which again costs more (Shafieian *et al.,* 2019). Therefore, by using nanofluid optimised performance from solar collectors can be achieved.

There are several papers available that describe the impact of nanofluid on the thermal characteristics of solar collectors. Ghaderian and Sidik (2017) Investigated the effect of the addition of aluminium oxide (Al_2O_3) in distilled water as nanofluid on ETSC with volume fractions of 0.03% and 0.06% for a flow rate of 20 to 60 liter/hrs. This study revealed that the maximum efficiency obtained from ETSC is 57.63%.

The experiment carried out by Sharafeldin *et al.* (2019) on metallic copper oxide (CuO) with different mass flow rates and volumetric concentrations explored that there is a 50% enhancement in output temperature and increment in heat energy by using ETSC. The silver water nanofluid study was conducted to find the thermal efficiency of thermo syphon heat pipe ETSC by Ozsoy and Corumlu (2018) investigated that there is a rise in efficiency of solar collector from 20.7 % to 40 % as compared to water.

Sabiha *et al.* (2015) prepared single-walled carbon nanotubes water-based nanofluid to test the effectiveness of ETSC with volumetric concentrations of 0.05%, 0.1%, and 0.2% under various flow rates and found out maximum efficiency of 93.43% can be achieved at volumetric concentration of 0.2%. Gan *et al.* (2018) examined titanium oxide (TiO_2) and distilled water nanofluid in addition to surfactant polyvinyl pyrrolidone (PVP) in ETSC and concluded that, the thermal conductivity of TiO_2 increases by 7.28%.

Ali *et al.* (2018) has critically reviewed various methods of fabrication of nanofluids, stability evaluation process, stability enhancements methods, and thermo physical properties of nanofluids. The current progress on nanofluids is also reported in this study.

Nevertheless, the experimental and numerical study on multiwalled carbon nanotube (MWCNT), TiO2, silicon dioxide (SiO2), and copper (Cu) with water as base fluid on ETSC revealed that the best thermal recovery is obtained from copper-water nanofluid and reduction in carbon dioxide (CO_2) and sulfur dioxide (SO_2). These experiments were performed by using various volumetric concentrations of the nanofluid and a numerical study was carried out by using the finite element method as reported by Yurddaş (2020).

By retaining nanofluid stability, the thermo physical properties of carbon-based nanofluid can be achieved with a low volumetric concentration of nanofluid samples (Nagarajan *et al.,* 2014). Recently, a study carried out on carbon nanotube nanofluids to improve ETSC efficiency investigated that thermal efficiency can be increased up to 56.7% to 66% when operating with water and volumetric concentration of 0.2% nanofluids (Mahbubul *et al.,* 2018). The peak outlet temperature was found to be 120.6 ^{o}C at the highest solar radiation. The thermal efficiency was found to be linear with the thermal loss function.

The primary goal of the present study is to enhance the thermal characteristics of ETSC by using GO/DI water-based nanofluid. However, GO nanoparticle has higher thermal conductivity hence, it is selected in this study. Ghosh *et al.* (2008) showed that higher thermal conductivity

material plays a significant role in heat carrying process and efficiency enhancement of solar collector. However, there are few researchers who studied the thermo physical properties of graphene and graphene-based materials. Several experiments were conducted to find the thermal performance and thermal efficiency of ETSC using graphene nanoplatelets-methanol nanofluid (Sarafraz & Safaei, 2019). The effect of various tilt angles of solar panels, filling ratio, and flow rates are also discussed in this study. The study by Iranmanesh *et al.* (2017) on graphene nanoplatelets in distilled water as base fluid investigated ETSC water heaters with 0.025, 0.5, 0.075, and 0.1 wt% concentration and mass flow rates of 0.5 lit/min, 1 lit/min, and 1.5 lit/min revealed that ETSC thermal efficiency increases up to 90.7% at a mass flow rate of 1.5 lit/min as compared to water.

The multilayer graphene-based nanofluids were analysed experimentally by using ETSC with and without parabolic concentrator. Natividade *et al.* (2019) explained that a parabolic concentrator increases mean efficiency by 298% as compared to without a concentrator. They used multilayer graphene in low volumetric fractions with a parabolic concentrator.

The above literature studies indicate that graphene-based material can be useful in increasing the thermal efficiency of solar collectors up to a greater extent hence GO is considered in this study as research work with evacuated tube heat pipe solar collectors.

II. MATERIALS AND METHOD

A. Synthesis of Nanofluid

1. Materials

Potassium permanganate ($KMNO_4$), Hydrogen chloride (HCl), hydrogen peroxide (H_2O_2), Sulphuric acid (H_2SO_4), graphite flakes, Phosphoric acid (H_3PO_4), and deionised water were used in the experimentation.

2. Synthesis of GO

There are several methods to synthesise graphene Oxide, including the hummers process, modified hummer's approach, and improved synthesis method. The modified hummers method was a commonly used method by researchers but the improved synthesis method is used for large-scale production of GO as it does not produces toxic gases (Marcano *et al.,* 2010). Initially, a mixture of Sulphuric acid (H_2SO_4) and Phosphoric acid (H_3PO_4) is prepared in 9:1 proportion followed by the addition of 3 gm. of graphite powder. The potassium permanganate ($KMNO_4$) of 18 gm. was added after a certain interval of time in the mixture and stirred (290 to 300 rpm) for 48 hrs.

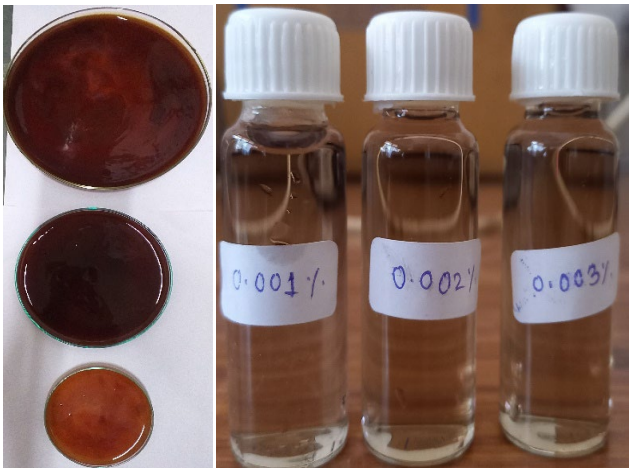

(a) (b)

Figure 1. Synthesis of GO (a) Dry GO sample, and (b) GO/DI samples.

The reaction mixture was cooled to room temperature and poured onto ice (1000 ml of water) with 30% hydrogen peroxide (H_2O_2) as the colour changed from dark black in a greenish shade to yellow. Then it is kept to settle for overnight. The solution was decanted, and the cake was washed with 640 ml of deionised water and 100 ml of Hydrogen chloride (HCl) to maintain the pH value of 7 and kept for drying.

The deionised water is used as base fluid with prepared graphene oxide and three different volumetric concentrations of samples 0.001%, 0.002%, and 0.003% were prepared as shown in Figure 1(b).

B. GO Nanoparticles Characterisation

1. X-ray diffraction (XRD) spectroscopy

The crystalline pattern of the GO sample was identified by X-ray diffraction spectroscopy (Krishnamoorthy *et al.,* 2013). The XRD (Bruker D8 Advance) was used to record X-ray diffraction patterns which were operated at 40 kV and 45 mA and the diffraction patterns were captured in the

range of 5° to 55° with a scan speed of 20°/min. Figure 2 shows the XRD test pattern of the GO sample which was used to find the purity and degree of oxidation.

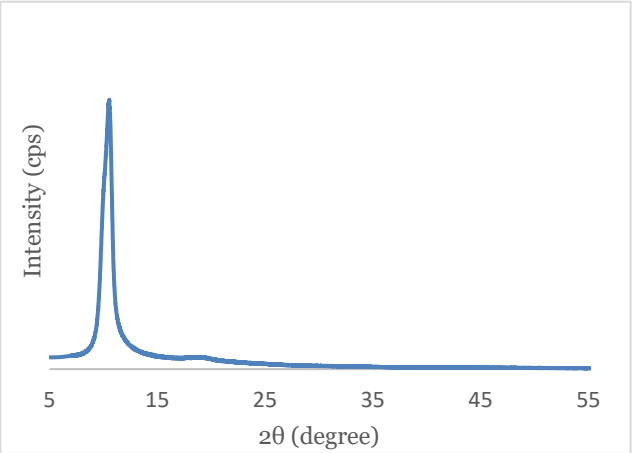

Figure 2. X-ray diffractogram.

A clear visible peak of 10.56° was observed at 2θ for GO samples which confirms the presence of GO. The associated parameters like inter-layer spacing (*dspace*), average crystallite size (*Dhkl*), average number of graphene layers (*n*), and in-plane crystallite size (*Lp*) were calculated from XRD (Stobinski *et al.,* 2014), and values are tabulated in Table 1. It confirms the incorporation of oxygen-based functional groups in between the graphene nanosheets of GO.

Table 1. Experimental parameters derived from XRD.

Technique	**XRD**				
Sample	2θ (deg.)	d_{space} (nm)	D*hkl* (nm)	Layers (n)	*Lp* (nm)
GO	10.56	0.8367	18.744	24	38.91

2. Morphology of synthesised GO

The morphology of graphene oxide is carried out by using scanning electron microscopy. Figure 3 shows a scanning electron microscopic image of graphene oxide.

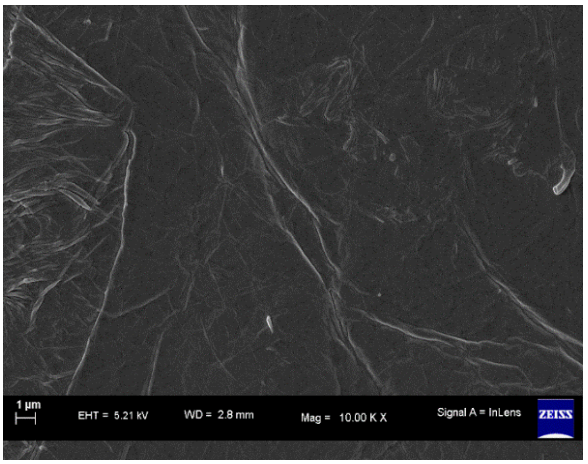

Figure 3. SEM Image.

Scanning electron microscope provides information about nanoparticle structure, combination, fracture surface, locality, and surface pollution. The average size of the nanoparticle can be found by using a scanning electron microscope (Esfahani *et al.,* 2016).

C. Nanofluid Stability

The main problem associated with nanofluid technology is its poor stability which significantly decreases the heat transfer rate. This is due to the intense van der walls forces of attraction between liquid molecules which form sedimentation and agglomeration (Hwang *et al.,* 2007), hence the evaluation of nanofluid stability becomes an important factor before testing in ETSC. The different techniques, including zeta potential analysis, spectral analysis method, sedimentation photography, and centrifugation process can be used to evaluate the stability of nanofluid. However, zeta potential analysis is the most commonly used method which provides a better estimation of the stability of nanofluid. Hence, in this work nanofluid stability is evaluated using the zeta potential method. Initially, zeta potential is carried out just after the preparation of samples and then after 30 days of preparation to study nanofluid's stability period.

The results of zeta potential analysis are plotted in Figure 4, which shows that the samples can be stable up to 30 days and the values ranging from (± 40 to 60) mV show good stability whereas values (± 30 to 40) mV confirm stable solution (Chakraborty & Panigrahi, 2020).

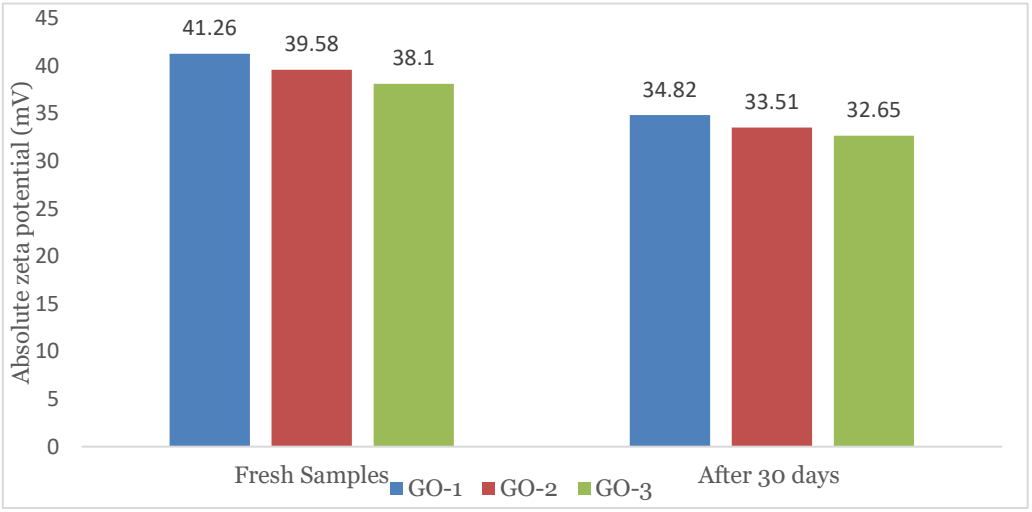

Figure 4. Stability evaluation by zeta potential method.

The high values of zeta potential (both positive and negative) of samples have a higher repulsive force which resists particles to come close to each other. It could be noted that sedimentation and agglomeration can take place if the particle and base fluid has major density difference even though zeta potential values are higher.

D. Thermo physical Properties of GO

The different volumetric concentration of nanoparticle affects the thermo physical characteristics of nanofluid (Safiei *et al.,* 2020). Therefore, thermal conductivity, viscosity, and specific heat capacity of nanofluid samples are evaluated at room temperature and the effect of different volumetric concentrations of nanofluid on thermo physical properties are depicted in Figures 5 and 6. An essential aspect that improves the thermal performance of the collector is an increase in thermal conductivity of nanofluid. This can be attributed to high thermal conductivity due to the insertion of high thermal conductive nanoparticles into a base fluid. From Figure 5, it is observed that as volumetric concentration increases, the thermal conductivity of nanofluid samples also increases. The total enhancement in thermal conductivity of 6.45%, 24.83%, and 42.9% at vol. conc. of 0.001%, 0.002%, and 0.003%, respectively are observed as compared to water.

Adding nanoparticles to the base fluid lowers the specific heat capacities of GO samples and it is expected that it increases as an increase in temperature at a fixed concentration. As shown in Figure 6, GO/DI water nanofluid's specific heat capacity decreases from 4.1 KJ/kg.k to 3.72 KJ/kg.k at a volumetric concentration of 0.003%. The reduction in the specific heat of GO nanofluid can be attributed to the lower heat capacity of nanoparticles (Hajjar, Rashidi & Ghozatloo 2014; Riazi *et al.* 2016). It is crucial to remember that, due to the higher thermal conductivity of nanofluid, there is an increase in the thermal performance of the collector by increasing temperature difference even though specific heat capacity decreases with a volumetric concentration of nanofluid which is discussed in the next section.

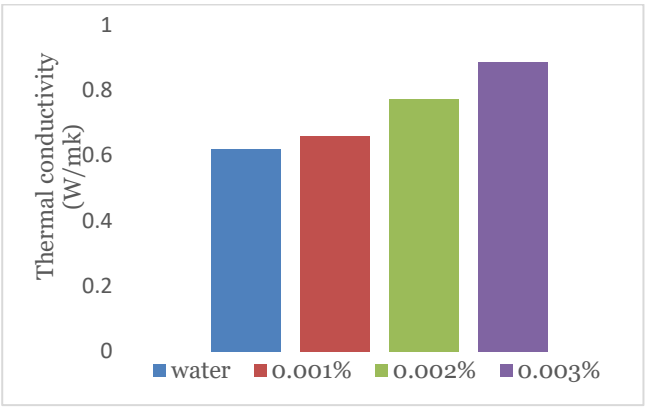

Figure 5. Thermal conductivity of samples at room temperature.

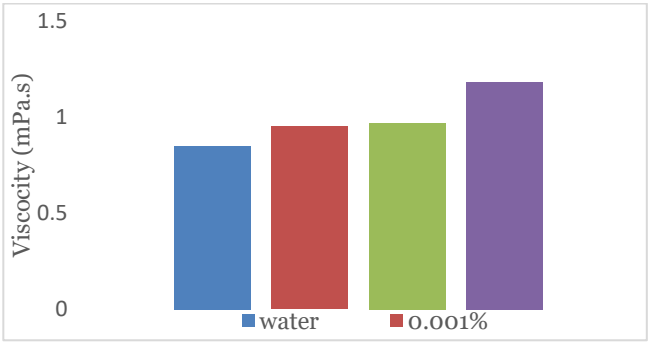

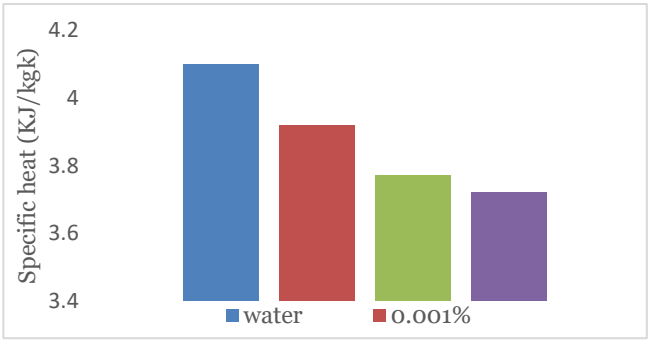

Figure 6. Viscosity and specific heat of samples at room temperature.

According to Figure 6, an increase in volumetric concentration increases the viscosity of GO samples. The possible reason is due to high specific area of GO results in an increase in resistance to flow and thereby an increase in viscosity of samples (Selvam *et al.,* 2016). The maximum increase in viscosity is observed to be 38.82% at 0.003% volumetric concentration as compared to water.

III. EXPERIMENTAL TEST SET UP AND PROCEDURE

The schematic of heat pipe ETSC is shown in Figure 7, which was used to carry out an experimental study on water and nanofluid samples. The detailed specification of the ETSC is summarised in Table 2.

Table 2. Specification of solar collector.

Specification	Dimension
Type of collector	Evacuated tube copper heat pipe solar collector
Tube diameter	58 mm
Tube length	1800 mm
Absorber Coating	Tinox energy Cu
Glass	Borosilicate 3.3
Aperture area	1.92 m²
Peak Power	1175 W
No of Tubes	20
Absorption coefficient	0.94
Emission coefficient	0.07
Absorber area	1.65 m²
Operating pressure	6 bar

The test setup was fabricated and tested in the solar site of Ratnagiri, Maharashtra (Lat.17.05°N; Long.73.56°E) with south facing of 40° tilt angle. The setup is a closed loop type and consists of a storage tank, heat exchanger, temperature sensors, flow control valve, pressure release valve, and hot water pump as shown in Figures 7 and 8.

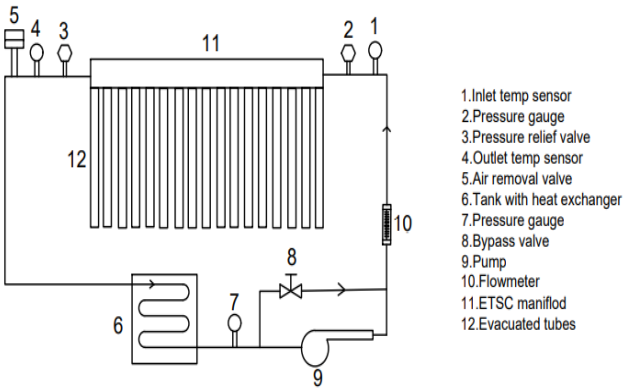

Figure 7. Schematic of test set up.

Figure 8. Actual test set up at testing site.

Initially, the water is fed to the system and then different nanofluid samples were used for testing with mass flow rates of 0.5 lit/min, 0.75 lit/min, and 1 lit/min. The experiments were carried out in the highest sunshine with a clear sky to get maximum benefit.

A. Efficiency Calculation

This section discusses the numerical computations needed to evaluate the thermal performance parameter of ETSC. The instantaneous efficiency of ETSC is calculated by the ratio of usable heat gain to total solar radiations received on the collector. According to (Lee & Baek, 2014), the efficiency of ETSC can be calculated by using Equation (1):

$$\eta = Qu/Qin = mCp(To - Ti)/AcG \quad (1)$$

Where m is mass flow rate, C_p is the specific heat capacity of fluid, T_o is outlet temperature of solar collector and T_i is inlet temperatures of solar collector, A_c is solar collector absorbance area, Q_u is useful heat gain by water, G is solar irradiance, Q_{in} is total energy incident on collector and η is an efficiency of ETSC. The useful heat gain (Qu) is calculated as:

$$Qu = m.Cp.(To - Ti) \quad (2)$$

However, useful heat gain is also be expressed as heat gain by fluid minus heat losses:

$$Q_u = A_C F_R [G(\tau\alpha) - U_L(T_i - T_a)] \quad (3)$$

Hence, rearranging Equations (1) and (3), the efficiency can be written as:

$$\eta = F_R(\tau\alpha) - F_R U_L(T_i - T_a) \quad (4)$$

And total energy incident on ETSC is calculated by:

$$Q_{in} = A_c.G \quad (5)$$

Based on the above Equations the thermal efficiency of ETSC can be calculated.

B. Uncertainty Analysis

According to (Anin Vincely & Natarajan, 2016), the standard error (SE) or uncertainty analysis is used to demonstrate measurement accuracy during experimentation and it is calculated by using Equation (6):

$$\delta\eta i/\eta i = [(\delta m/m)^2 + (\delta Cp/Cp)^2 + (\delta(To-Ti)/(To-Ti))^2 + (\delta Ac/Ac)^2 + (\delta G_T/G_T)^2]^{0.5} \quad (6)$$

The efficiency of ETSC is calculated by measuring mass flow rate, specific heat capacities, temperature difference, collector area, and solar radiations. Hence the errors in the parameters must be considered in experimental work. The values of standard error during experimental work are listed in following Table 3.

Table 3. Uncertainty analysis of measurement.

Parameter	**Standard error**
Flow rate, L/hr.	± 1%
Specific heat capacity,	±0.2%
Temperature difference, ^oC	±0.5%
Solar radiation, W/m^2	±2%
Solar collector area, m^2	±0.13%

Therefore, the maximum standard error in the measurement of thermal efficiency in this presented work is 2.30%.

IV. RESULTS AND DISCUSSION

The experimental test was conducted during the month of January to May, for the period between 9.30 am to 4.30 pm in a day. The readings has been taken at different time intervals as shown in Figure 9 and average reading values were considered for plotting the graph. The different weather conditions were measured like ambient temperature and solar radiations and are plotted in Figure 9. The maximum solar radiations of 807 W/m^2 and the surrounding temperature of 37 ^oC were recorded at 13.00 pm. After 13.00 pm solar radiation and ambient temperature start decreasing.

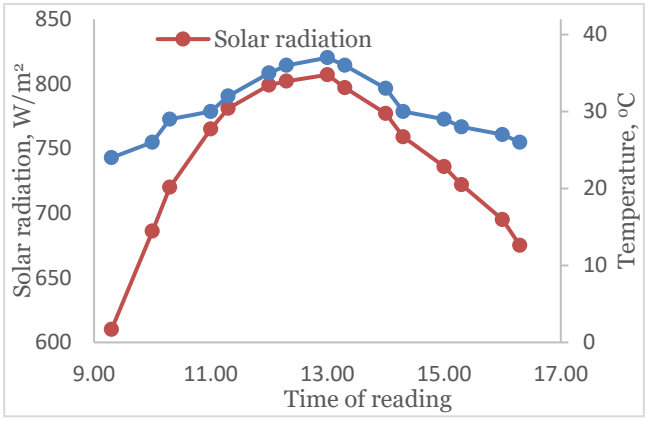

Figure 9. Solar radiation data, ambient temperature vs. time of reading graph.

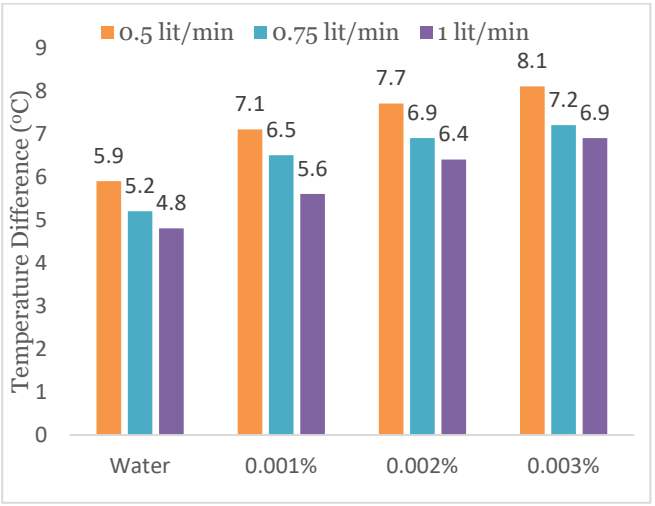

Figure 10. Temperature difference versus volumetric concentration.

A. Temperature Difference

The temperature difference is the most important parameter to investigate the thermal performance of ETSC. It is a difference in inlet fluid temperature and temperature of the fluid leaving collector. As the thermal efficiency of the collector is directly affected by temperature difference hence it becomes a significant factor to study. The temperature difference for pure water and nanofluid volumetric concentrations is displayed in Figure 10. The temperature difference for water is found to be 5.9 °C at a mass flow rate of 0.5 lit/min and it gets decreases to 5.2 °C and 4.8 °C at a mass flow rate of 0.75 lit/min and 1 lit/min, respectively. Further increase of mass flow rate, increases temperature difference when compared to water. The temperature difference for volumetric concentration of 0.001% are recorded as 7.1 °C, 6.5 °C and 5.6 °C at mass flow rate of 0.5 lit/min, 0.75 lit/min, and 1 lit/min, respectively. Similarly, using volumetric concentration of 0.002% nanofluid sample, the temperature difference values decrease as 7.7 °C, 6.9 °C and 6.4 °C at flow rate of 0.5 lit/min, 0.75 lit/min, and 1 lit/min, respectively. The higher temperature difference values are obtained at a volumetric concentration of 0.003%. These values increase up to 8.1 °C, 7.2 °C and 6.9 °C at mass flow rate of 0.5 lit/min, 0.75 lit/min, and 1 lit/min, respectively.

According to Figure 10, the temperature difference is higher in nanofluids than in pure water because of higher nanofluid's thermal conductivity as compared to water. This improvement of nanofluid's thermal conductivity is significantly influenced by the Brownian motion of particles (Sharafeldin & Gróf, 2018). As temperature increases, a collision between nanoparticles in the fluid also increases which is responsible for the enhancement in thermal conductivity. With the rise in temperature, collision between base fluid molecules and nanoparticles is rapid which improves the thermal conductivity of nanofluid (Chopkar *et al.,* 2008). Therefore, the temperature difference increases as the thermal conductivity of nanofluid increases.

B. The Useful Heat Gain

Figure 11 depicts, the change in volumetric concentrations and mass flow rate's effect on the amount of heat absorbed by the water. This useful heat gain value indicates the amount of energy absorbed in working fluid when passing through the collector and it is calculated by using Equations (3) and (4). The useful heat gain depends on various parameters like mass flow rate, density, specific heat, temperature difference, heat removal factor, absorber area, etc. When water is used in solar collector, the heat gain values are found out as 198 W, 278 W and 342 W at a mass flow rate of 0.5 lit/min, 0.75 lit/min, and 1 lit/min, respectively. These heat gain values increase when nanofluid samples are used in the solar collector and the values

increases to 238 W, 347 W and 398 W at a mass flow rate of 0.5 lit/min, 0.75 lit/min, and 1 lit/min, respectively using a volumetric concentration of 0.001%. Further, increase in the volumetric concentration of nanofluid to 0.002%, there is an increase in heat gain values to 258 W, 368 W and 455 W at a mass flow rate of 0.5 lit/min, 0.75 lit/min, and 1 lit/min, respectively and the higher values of heat gain are recorded as 271 W, 384 W and 491 W at a mass flow rate of 0.5 lit/min, 0.75 lit/min, and 1 lit/min, respectively at a volumetric concentration of 0.003%.

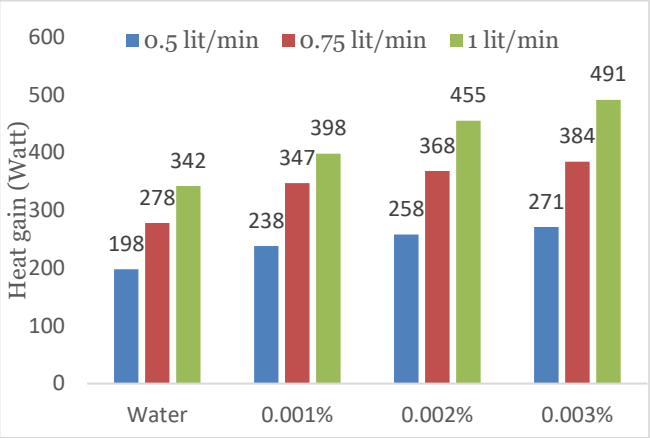

Figure 11. Heat gain versus volumetric concentration.

The maximum enhancement in useful heat gain of 43.56% is achieved in the volumetric concentration of 0.003% at 1 lit/min mass flow rate when compared to water. The useful heat gain values increases by an increase in the volumetric concentration of nanofluid and mass flow rate because the temperature of returning nanofluid is maximum than water therefore temperature difference values increases which increases heat gain (Sharafeldin & Gróf, 2019). Similarly, adding more nanoparticles into base fluid results in an increase in density and decreases specific heat capacity but temperature difference values increase. This increase in temperature difference values increases the useful heat gain (Kaya *et al.,* 2018).

C. Thermal Efficiency Using Water and Nanofluid

The main intention of the work is to enhance the thermal efficiency of ETSC by using GO/DI nanofluid. This section describes the effect of different volumetric concentrations and mass flow rates on thermal efficiency. Also, a comparative study of water and different nanofluid samples is depicted in Figure 12. The solar collector efficiency using water and nanofluid samples as working fluid is calculated by using Equation (1). From the figure it is clear that maximum efficiency is obtained at 13.00 pm for both water and nanofluid samples. This is due to maximum solar radiation and temperature difference. After 13.00 pm efficiency decreases as solar radiation decreases. This is due to the fact that, as solar radiation increases the collector absorbs more heat energy which increases thermal efficiency. Also, it confirms that solar collectors with nanofluid have better efficiency than water as base fluid and maximum improvement by using nanofluid is obtained at the highest solar radiation because the thermal conductivity increases with an increase in temperature (Zambolin & Del Col, 2010).

1. Mass flow rate effect

In this work, 0.5 lit/min, 0.75 lit/min, and 1 lit/min mass flow rates were examined and their effects on thermal efficiency are depicted in Figure 12 (a-c). For the mass flow rate of 0.5 lit/min, the maximum efficiencies are found to be 15.1, 17.8, 19.9 and 22.3% for water, 0.001%, 0.002%, and 0.003% volumetric concentration, respectively. Further increase of mass flow rate to 0.75 lit/min, there is a significant increase in thermal efficiencies. These values are increased up to 20.2, 25.7, 27.6 and 30.4% for water, 0.001%, 0.002%, and 0.003% volumetric concentration, respectively. The maximum values of thermal efficiencies are found as 25.7, 29.9, 34.2 and 37.1 % for water, 0.001%, 0.002%, and 0.003% volumetric concentration, respectively at a mass flow rate of 1 lit/min. The maximum enhancement in the thermal efficiency is 44.35% obtained at a mass flow rate of 1 lit/min for 0.003% volumetric concentration of nanofluid when compared with water.

Table 4. Results of water as working fluid in ETSC.

Flow rate (lit/min)	Maximum efficiency (%)	Average efficiency (%)
0.5	15.1	9.54
0.75	20.2	11.04
1	25.7	12.32

From Table 4, it can be noted that as the mass flow rate increases, the thermal efficiency of the collector also

increases. Using pure water as a base fluid, the efficiency increases from 15.1% to 25.7% for the mass flow rate of 0.5 lit/min to 1 lit/min, respectively and the average efficiency increased from 9.54% to 12.32% for the mass flow rate of 0.5 lit/min to 1 lit/min, respectively.

It is evident from these results that, ETSC efficiency increased as the mass flow rate is increased. The possible reason behind this is, at the low mass flow rate, working fluid temperature increases because working fluid remains in the solar collector for a longer period of time than in a high mass flow rate which is held responsible for more radiation loss and convection. However at the high mass flow rate, the nanofluid remains in the solar collector for a short period of time hence thermal losses decreases and collector efficiency gets increases (Zhang & Yamaguchi, 2008). One more reason behind this behaviour is, as mass flow rate increases turbulence speed up and mixing between the fluid layers is rapid which increases heat transfer rate in fluid and the thermal efficiency of ETSC is increased (Yousefi *et al.,* 2012).

2. Effect of nanofluid volumetric concentration

The three different volumetric concentrations of 0.001%, 0.002%, and 0.003% GO/DI water were prepared and tested in ETSC. Figure 12 (a-c) shows the thermal efficiency of ETSC with time for various mass flow rates.

Table 5. Mass flow rate effect on efficiency.

Vol. conc.	Efficiency	Mass flow rate		
		0.5 lit/min	0.75 lit/min	1 lit/min
0.001 %	Maximum	17.8 %	25.7%	29.9%
	Average	11.64 %	13.35 %	15.64 %
0.002 %	Maximum	19.4 %	27.6 %	34.2 %
	Average	12.39 %	14.42 %	17.56 %
0.003 %	Maximum	20.6 %	28.8 %	37.1 %
	Average	13.92 %	15 %	19.16 %

According to Table 5, for the 0.001%, volumetric concentration of the sample maximum efficiency increases from 17.8 % to 29.9 % as the mass flow rate increases from 0.5 lit/min to 1 lit/min, respectively. The thermal efficiency of the solar collector increases as volumetric concentration increases. The maximum efficiency of 19.4%, 27.6 % and 34.2 % found out for 0.002% sample at mass flow rate of 0.5 lit/min, 0.75 lit/min, and 1 lit/min, respectively. The highest maximum efficiency is obtained as 37.1 % at a mass flow rate of 1 lit/min for 0.003% volumetric concentration. The lowest average efficiency is gained as 11.64 % for 0.001% vol. conc. at 0.5 lit/min mass flow rate whereas the highest average efficiency of 19.16 % is obtained for 0.003% vol. conc. sample at 1 lit/min.

It is clear that the efficiency of ETSC increased with an increase in volumetric concentrations from 0.001% to 0.003%. It is also seen that use of 0.003% vol. conc. Sample leads to high performance than water as a working fluid. This is possible due to the highest useful heat gain of nanofluid compared to water. The insertion of nanoparticles in water as base fluid enhances absorptivity and thermo physical properties like an increase in thermal conductivity, increase in absorptivity and reduces specific heat capacity which is responsible for the enhancement in the ETSC efficiency.

The enhancement in a heat transfer rate of working fluid is because of the higher heat capacity and thermal conductivity of nanoparticles than water. In addition, the damping coefficient of working fluid plays a vital role in heat transfer as energy absorption increases with an increase in the volumetric concentration of nanofluid. More and more incoming solar radiation get absorbed in a high volumetric concentration of nanofluid (Michael & Iniyan, 2015).

Also, it can be concluded that solar collector efficiency increases as solar radiation increases and vice versa. As solar radiation increases more heat gets absorbed in the collector which enhances thermal efficiency and as solar radiation starts decreasing less amount of heat is absorbed by the fluid which decreases thermal efficiency. Hence maximum efficiency can be achieved during noon time when solar radiations are maximum.

The Table 6 shows comparative study of current research work and previous studies on ETSC to improve thermal efficiency. It could be noted that collector capacity and environmental factors are different for each study. However, the current study shows maximum enhancement in thermal efficiency of ETSC due to high thermal conductivity of GO.

Table 6. Comparative study.

Reference	Nanofluid	Specification	Thermal efficiency
(Iranmanesh *et al.*, 2017)	GNP	Vol. Con. 0.025% Flow Rate 1 lit/min	3%
(Ghaderian *et al.*, 2017)	CuO/H2O	Vol. Con. 0.03% Flow Rate 1 lit/min	32%
(Sharafeldin & Gróf, 2018)	CeO2	Vol. Con 0.03% Flow Rate 0.83 lit/min	34%
(Natividade *et al.*, 2019)	MLG	Vol. Con 0.025% Flow Rate 0.067 lit/min	24.3%
Present study	GO/DI	Vol. Con 0.003% Flow Rate 1 lit/min	37.1%

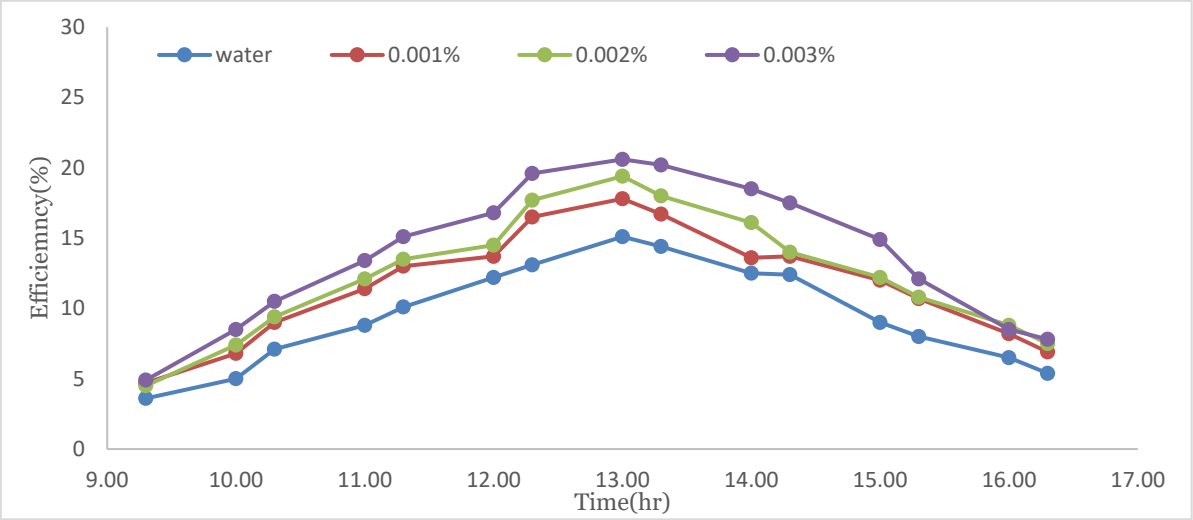

(a)

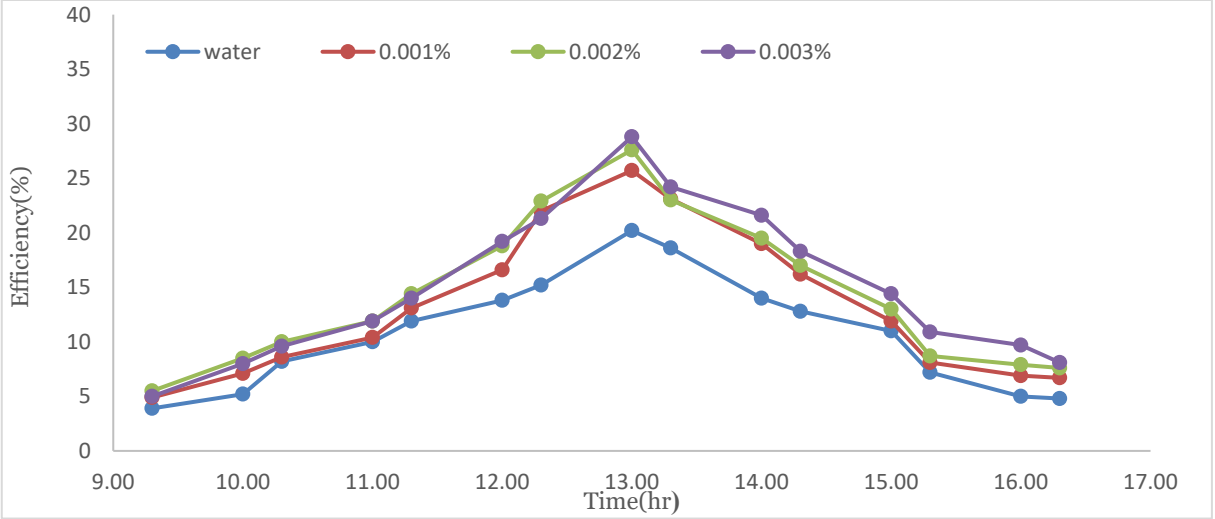

(b)

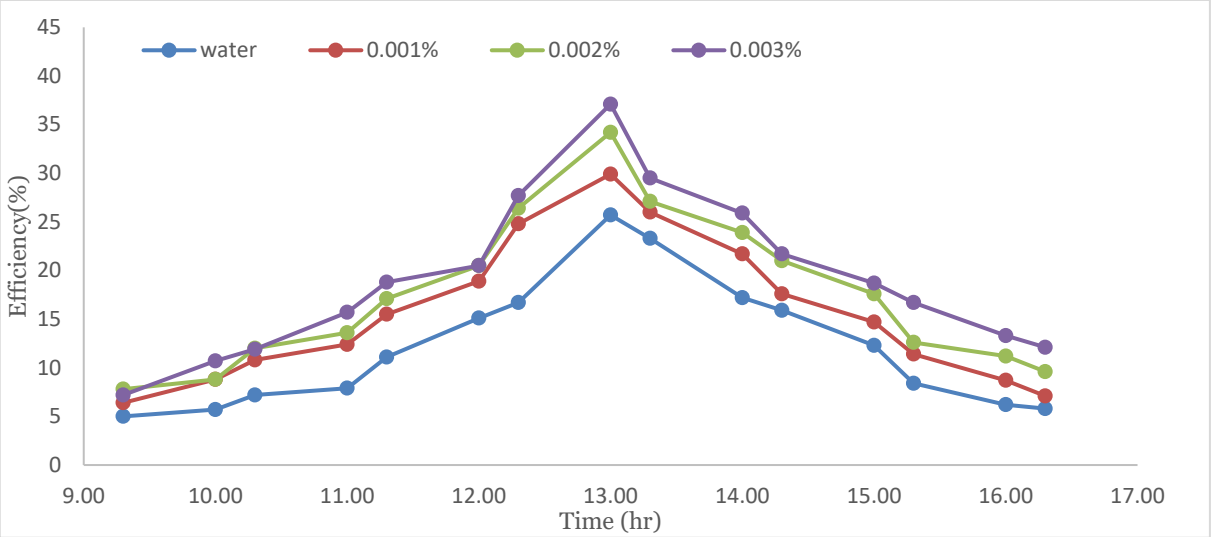

(c)

V. CONCLUSION

The experimental study was carried out on heat pipe ETSC by using GO/DI water nanofluid. The GO/DI water nanofluid was prepared and stability was checked. It was found stable for up to 30 days with no sedimentation. The pure water and GO/DI water samples of 0.001%, 0.002%, and 0.003% were tested in the ETSC test set up with a mass flow rate of 0.5 lit/min, 0.75 lit/min, and 1 lit/min. The various thermal metrics are found including temperature difference, beneficial heat gain and thermal efficiency. The maximum temperature difference of 8.1^{o}C was found for 0.003% vol. conc. at 0.5 lit/min. The maximum increase in useful heat gain of 43.56% was obtained for a volumetric concentration of 0.003% at mass flow rate of 1 lit/min. The water was observed to have maximum collector efficiency of 25.7% at a mass flow rate of 1 lit/min whereas the highest ETSC efficiency of 37.1% was observed for nanofluid with 0.003% vol. conc. at a mass flow rate of 1 lit/min. It is concluded that solar collector efficiency depends on solar radiation and mass flow rate.

VI. ACKNOWLEDGEMENT

The authors would like to acknowledge the kind support of the Department of Physics, ICT Mumbai.

Declaration of Conflicting Interest

The authors declare that they have no conflicts of interest.

VII. REFERENCES

Ahmed, A, Baig, H, Sundaram, S & Mallick, TK 2019, 'Use of Nanofluids in Solar PV/Thermal Systems', International Journal of Photoenergy, vol. 2019, p. e8039129.

Ali, N, Amaral Teixeira, J & Addali, A 2018, 'A Review on Nanofluids: Fabrication, Stability, and Thermophysical Properties', Journal of Nanomaterials, vol. 2018. doi: 10.1155/2018/6978130.

Anin Vincely, D & Natarajan, E 2016, 'Experimental investigation of the solar FPC performance using graphene oxide nanofluid under forced circulation', Energy Conversion and Management, vol. 117, pp. 1–11.

Chakraborty, S & Panigrahi, PK 2020, 'Stability of nanofluid: A review', Applied Thermal Engineering, vol. 174, p. 115259.

Chopkar, M, Sudarshan, S, Das, PK & Manna, I 2008, 'Effect of Particle Size on Thermal Conductivity of Nanofluid', Metallurgical and Materials Transactions A: Physical Metallurgy and Materials Science, vol. 39, pp. 1535–1542.

Dehaj, MS & Mohiabadi, MZ 2019, 'Experimental investigation of heat pipe solar collector using MgO nanofluids', Solar Energy Materials and Solar Cells, vol. 191, pp. 91–99.

Esfahani, MR, Languri, EM & Nunna, MR 2016, 'Effect of particle size and viscosity on thermal conductivity enhancement of graphene oxide nanofluid', International Communications in Heat and Mass Transfer, vol. 76, pp. 308–315.

Gan, YY, Ong, HC, Ling, TC, Zulkifli, NWM, Wang, C-T & Yang, Y-C 2018, 'Thermal conductivity optimization and entropy generation analysis of titanium dioxide nanofluid in evacuated tube solar collector', Applied Thermal Engineering, vol. 145, pp. 155–164.

Ghaderian, J & Sidik, NAC 2017, 'An experimental investigation on the effect of Al2O3/distilled water nanofluid on the energy efficiency of evacuated tube solar collector', International Journal of Heat and Mass Transfer, vol. 108, pp. 972–987.

Ghosh, S, Calizo, I, Teweldebrhan, D, Pokatilov, E, Nika, D, Balandin, A, Bao, W, Miao, F & Lau, J 2008, 'Extremely High Thermal Conductivity of Graphene: Prospects for Thermal Management Applications in Nanoelectronic Circuits', Applied Physics Letters, vol. 92, pp. 151911–151911. doi: 10.1063/1.2907977.

Hajjar, Z, Rashidi, A morad & Ghozatloo, A 2014, 'Enhanced thermal conductivities of graphene oxide nanofluids', International Communications in Heat and Mass Transfer, vol. 57, pp. 128–131.

Hwang, Y-J, Lee, JK, Lee, CH, Jung, YM, Cheong, SI, Lee, CG, Ku, BC & Jang, S 2007, 'Stability and Thermal Conductivity Characteristics of Nanofluids', Thermochimica Acta, vol. 455, pp. 70–74.

Iranmanesh, S, Ong, HC, Ang, BC, Sadeghinezhad, E, Esmaeilzadeh, A & Mehrali, M 2017, 'Thermal performance enhancement of an evacuated tube solar collector using graphene nanoplatelets nanofluid', Journal of Cleaner Production, vol. 162, pp. 121–129.

Jayanthi, N, Suresh Kumar, R, Karunakaran, G & Venkatesh, M 2020, 'Experimental investigation on the thermal performance of heat pipe solar collector (HPSC)', Materials Today: Proceedings, vol. 26, pp. 3569–3575.

Jouhara, H, Chauhan, A, Nannou, T, Almahmoud, S, Delpech, B & Wrobel, LC 2017, 'Heat pipe based systems - Advances and applications', Energy, vol. 128, pp. 729–754.

Kadhim, S & Ibrahim, O 2021, 'Improving the Thermal Efficiency of Flat Plate Solar Collector Using Nano-Fluids as a Working Fluids: A Review', Iraqi Journal of Industrial Research, vol. 8.

Kaya, H, Arslan, K & Eltugral, N 2018, 'Experimental investigation of thermal performance of an evacuated U-Tube solar collector with ZnO/Etylene glycol-pure water nanofluids', Renewable Energy, vol. 122, pp. 329–338.

Krishnamoorthy, K, Veerapandian, M, Yun, K & Kim, S-J 2013, 'The chemical and structural analysis of graphene oxide with different degrees of oxidation', Carbon, vol. 53, pp. 38–49. doi: 10.1016/j.carbon.2012.10.013.

Lee, K & Baek, N 2014, 'A Modified Efficiency Equation of Solar Collectors', Energy Procedia, vol. 48, pp. 145–149.

Lee, M, Shin, Y & Cho, H 2021, 'Theoretical study on performance comparison of various solar collectors using binary nanofluids', Journal of Mechanical Science and Technology, vol. 35, no. 3, pp. 1267–1278.

Mahbubul, IM, Khan, MMA, Ibrahim, NI, Ali, HM, Al-Sulaiman, FA & Saidur, R 2018, 'Carbon nanotube nanofluid in enhancing the efficiency of evacuated tube solar collector', Renewable Energy, vol. 121, pp. 36–44.

Marcano, D, Kosynkin, D, Berlin, J, Sinitskii, A, Sun, Z, Slesarev, A, Alemany, L, Lu, W & Tour, J 2010, 'Improved synthesis of graphene oxide ACS Nano 4:4806-4814', ACS nano, vol. 4, pp. 4806–4814.

Michael, JJ & Iniyan, S 2015, 'Performance of copper oxide/water nanofluid in a flat plate solar water heater under natural and forced circulations', Energy Conversion and Management, vol. 95, pp. 160–169.

Nagarajan, PK, Subramani, J, Suyambazhahan, S & Sathyamurthy, R 2014, 'Nanofluids for Solar Collector Applications: A Review', Energy Procedia, vol. 61, pp. 2416–2434.

Natividade, PSG, de Moraes Moura, G, Avallone, E, Bandarra Filho, EP, Gelamo, RV & Gonçalves, JC de SI 2019, 'Experimental analysis applied to an evacuated tube solar collector equipped with parabolic concentrator using multilayer graphene-based nanofluids', Renewable Energy, vol. 138, pp. 152–160.

Ozsoy, A & Corumlu, V 2018, 'Thermal performance of a thermosyphon heat pipe evacuated tube solar collector using silver-water nanofluid for commercial applications', Renewable Energy, vol. 122, pp. 26–34.

Riazi, H, Murphy, T, Webber, GB, Atkin, R, Tehrani, SSM & Taylor, RA 2016, 'Specific heat control of nanofluids: A

critical review', International Journal of Thermal Sciences, vol. 107, pp. 25–38.

Sabiha, MA, Saidur, R, Hassani, S, Said, Z & Mekhilef, S 2015, 'Energy performance of an evacuated tube solar collector using single walled carbon nanotubes nanofluids', Energy Conversion and Management, vol. 105, pp. 1377–1388. doi: 10.1016/j.enconman.2015.09.009.

Sabiha, MA, Saidur, R, Mekhilef, S & Mahian, O 2015, 'Progress and latest developments of evacuated tube solar collectors', Renewable and Sustainable Energy Reviews, vol. 51, pp. 1038–1054.

Safiei, W, Rahman, MM, Kulkarni, R, Ariffin, MN & Malek, ZAA 2020, 'Thermal Conductivity and Dynamic Viscosity of Nanofluids: A Review', Journal of Advanced Research in Fluid Mechanics and Thermal Sciences, vol. 74, no. 2, pp. 66–84.

Sarafraz, MM & Safaei, MR 2019, 'Diurnal thermal evaluation of an evacuated tube solar collector (ETSC) charged with graphene nanoplatelets-methanol nano-suspension', Renewable Energy, vol. 142, pp. 364–372.

Selvam, C, Lal, DM & Harish, S 2016, 'Thermal conductivity enhancement of ethylene glycol and water with graphene nanoplatelets', Thermochimica Acta, vol. 642, pp. 32–38.

Shafieian, A, Khiadani, M & Nosrati, A 2019, 'Thermal performance of an evacuated tube heat pipe solar water heating system in cold season', Applied Thermal Engineering, vol. 149, pp. 644–657.

Shafieian, A, Parastvand, H & Khiadani, M 2020, 'Comparative and performative investigation of various data-based and conventional theoretical methods for modelling heat pipe solar collectors', Solar Energy, vol. 198, pp. 212–223.

Sharafeldin, MA & Gróf, G 2018, 'Evacuated tube solar collector performance using CeO2/water nanofluid', Journal of Cleaner Production, vol. 185, pp. 347–356.

Sharafeldin, MA & Gróf, G 2019, 'Efficiency of evacuated tube solar collector using WO3/Water nanofluid', Renewable Energy, vol. 134, pp. 453–460.

Sharafeldin, MA, Gróf, G, Abu-Nada, E & Mahian, O 2019, 'Evacuated tube solar collector performance using copper nanofluid: Energy and environmental analysis', Applied Thermal Engineering, vol. 162, p. 114205.

Stobinski, L, Lesiak, B, Malolepszy, A, Mazurkiewicz, M, Mierzwa, B, Zemek, J, Jiricek, P & Bieloshapka, I 2014, 'Graphene oxide and reduced graphene oxide studied by the XRD, TEM and electron spectroscopy methods', Journal of Electron Spectroscopy and Related Phenomena, vol. 195. doi: 10.1016/j.elspec.2014.07.003.

Tsai, T-H, Chien, H-T & Chen, P-H 2011, 'Improvement on thermal performance of a disk-shaped miniature heat pipe with nanofluid', Nanoscale research letters, vol. 6, p. 590.

Wole-osho, I, Okonkwo, EC, Abbasoglu, S & Kavaz, D 2020, 'Nanofluids in Solar Thermal Collectors: Review and Limitations', International Journal of Thermophysics, vol. 41, no. 11, p. 157.

Yousefi, T, Veisy, F, Shojaeizadeh, E & Zinadini, S 2012, 'An experimental investigation on the effect of MWCNT-H2O nanofluid on the efficiency of flat-plate solar collectors', Experimental Thermal and Fluid Science, vol. 39, pp. 207–212.

Yurddaş, A 2020, 'Optimization and thermal performance of evacuated tube solar collector with various nanofluids', International Journal of Heat and Mass Transfer, vol. 152, p. 119496.

Zambolin, E & Del Col, D 2010, 'Experimental analysis of thermal performance of flat plate and evacuated tube solar collectors in stationary standard and daily conditions', Solar Energy, vol. 84, no. 8, pp. 1382–1396.

Zhang, XR & Yamaguchi, H 2008, 'An experimental study on evacuated tube solar collector using supercritical CO2', Applied Thermal Engineering, vol. 28, no. 10, pp. 1225–1233.

Zheng, D, Zhai, Z, Wang, W, Wang, J, Vujanović, M & Sundén, B 2022, 'Investigation on thermal performance of electric heaters with nanofluids', Fuel, vol. 320, p. 123966.